

Synthesis and structural characteristics of $\text{Co}_{1-x}\text{Cu}_x\text{Fe}_2\text{O}_4$ magnetic ferrite nanoparticles using hydrothermal technique

Mohanad A. Aswad and Falah A-H. Mutlak

Department of Physics, College of Science, University of Baghdad

E-mail: falah.mutlak5@gmail.com

Abstract

In this work, copper substituted cobalt ferrite nanoparticles with chemical formula $\text{Co}_{1-x}\text{Cu}_x\text{Fe}_2\text{O}_4$ ($x=0, 0.3, \text{ and } 0.7$), has been synthesized via hydrothermal preparation method. The structure of the prepared materials was characterized by X-ray diffraction (XRD). The (XRD) patterns showed single phase spinel ferrite structure. Average crystallite size (D), lattice constant (a), and crystal density (dx) have been calculated from the most intense peak (311). Comparative standardization also performed using smaller average particle size (D) on the XRD patterns of as-prepared ferrite samples in order to select most convenient hydrothermal synthesis conditions to get ferrite materials with smallest average particle size.

Key words

Ferrite nanoparticles, hydrothermal synthesis, cobalt ferrite, Scherrer formula.

Article info.

Received: Sep. 2018

Accepted: Oct. 2018

Published: Mar. 2019

تحضير و تشخيص الخواص التركيبية لدقائق $\text{Co}_{1-x}\text{Cu}_x\text{Fe}_2\text{O}_4$ الفريت المغناطيسية النانوية باستخدام تقنية الهيدروحرارية

مهند عبد الكريم اسود و فلاح عبد الحسن مطلق

قسم الفيزياء، كلية العلوم، جامعة بغداد

الخلاصة

في هذا العمل، جسيمات كوبالت الفرات النانوية المطعمة بأيونات النحاس قد تم تحضيرها وبتركيز مختلفة حسب العلاقة $\text{Co}_{1-x}\text{Cu}_x\text{Fe}_2\text{O}_4$ حيث ان ($x=0, 0.3, 0.7$) حيث تم التحضير باستخدام طريقة الهيدروحرارية. الخواص التركيبية للمواد المحضرة قد تم فحصها باستخدام تقنية حيود الاشعة السينية XRD نتائج هذا الفحص بينت ظهور الطور المغزلي الاحادي الخاص بتركيب الفريت. معدل الحجم البلوري للجسيم (D) وثابت الشبيكة (a) و الكثافة البلورية (dx) قد تم حسابها من بيانات حيود الاشعة السينية باستخدام القمة (311). بالاضافة الى ذلك قد تم استخدام المعايير عن طريق المقارنة من اجل معرفة شروط التحضير الامثل بطريقة الهيدروحرارية وكذلك من اجل الحصول على عينات الفريت و بحجم بلوري اصغر.

Introduction

Recent years, there is a large and wondering interest in the magnetic nanoparticles thanks to their fascinating unique chemical, thermal and magnetic properties [1]. Among these magnetic nanoparticles, spinel ferrite nanocrystals with the general formula MFe_2O_4 (where M is a divalent cation of Co, Ni, Mn, Mg or Zn) are very important materials because of their interesting electrical and magnetic properties with high

chemical and thermal stabilities [2], Which make them suitable for several disciplines like magnetic fluids [3], catalysis [4], biotechnology/biomedicine [5], magnetic resonance imaging [6], data storage devices [7], transformers, disk recording, electric generators, etc. [8]. Spinal cobalt ferrite (CoFe_2O_4) has been widely interested and studied due to high electromagnetic performance, mechanical hardness, excellent chemical stability, and high cubic

magneto-crystalline anisotropy [9]. Substitution of transition metal like Zn^{+2} , Cu^{+2} , and Ni^{+2} ion in Co-ferrite nanoparticles allows variation in their properties and tune ability for specific application, so the general formula will be as $CoMFe_2O_4$ where M is the transition metal ions [10]. Methods widely used for the synthesis of magnetic cobalt ferrite are: co-precipitation [11], hydrothermal [12], reverse micelles [13], sol-gel processing and etc. [14]. Among these methods, hydrothermal synthesis has attracted great interest because it is a promising route to produce highly crystallized, weakly agglomerated powders having a narrow size distribution [15]. The aim of this work is to synthesis the copper substituted cobalt ferrite nanoparticles with formula $Co_{1-x}Cu_xFe_2O_4$ where ($x=0, 0.3, \text{ and } 0.7$) via hydrothermal route, Materials characterization by X-ray diffractometer, study and analyze structural properties, also use comparative standardization to get most optimum ferrite samples with smallest average particle size.

Experimental procedure

1. Synthesis process

All reagents were of analytic grade, ultra-pure, and used as received without further purification, including cobalt nitrate hexahydrate ($Co(NO_3)_2 \cdot 6H_2O$) manufactured by (General Co., England), Cupric sulfate pentahydrate ($CuSO_4 \cdot 5H_2O$) manufactured by (Fluka Co., Switzerland), Ferric nitrate nonahydrate ($Fe(NO_3)_3 \cdot 9H_2O$) manufactured by (Scharlau Co., Spain) and sodium hydroxide pellets (NaOH) manufactured by (G.T Baker Co., Sweden).

The copper substituted cobalt ferrite nanoparticles prepared by hydrothermal reaction in distilled water. The aqueous salt solutions of

cobalt nitrate, cupric sulfate, and ferric nitrate are in molar ratio (1:1:2) dissolved in 50 ml of distilled water on a magnetic stirrer at moderate speed and temperature of ($65^\circ C$), then these solutions mixed together in a Pyrex beaker under constant stirrer for 15 minutes. (1.5M) of sodium hydroxide (NaOH) solution was add dropwise to the mixed metal solution under vigorous stirring for half an hour and the same temperature of ($65^\circ C$), in the meanwhile we checked the pH which should be approximately equal to 12. Experimental set up of this procedure can be illustrated in the Fig.1.

The resulting suspension was then poured into a Teflon-lined autoclave and hydrothermally heated at a special temperature for a certain time (hydrothermal conditions). After that, the autoclave was cooled to room temperature and the product was filtered, washed with deionized water and ethanol for three times in sequence to remove all soluble salts, and dried at ambient temperatures in order to get a black ferrite powder which would be ready for characterization. Note that in the preparation of $CoFe_2O_4$ ($x=0$) cupric sulfate hadn't been used and its solution eliminate from the Fig.1.

2. Hydrothermal conditions

The synthesis procedure involve prepare, for each of the three ferrite compound $Co_{1-x}Cu_xFe_2O_4$, ($x=0, x=0.3, \text{ and } 0.7$), three identical samples and named as sample-1, sample-2, and sample-3 for the $CoFe_2O_4$, sample-4, sample-5 and sample-6, for the $Co_{0.7}Cu_{0.3}Fe_2O_4$, sample-7, sample-8 and sample-9 for the $Co_{0.3}Cu_{0.7}Fe_2O_4$. Each sample was kept in the oven for time (t) and temperatures (T). These conditions can be shown by the diagram in Fig.2.

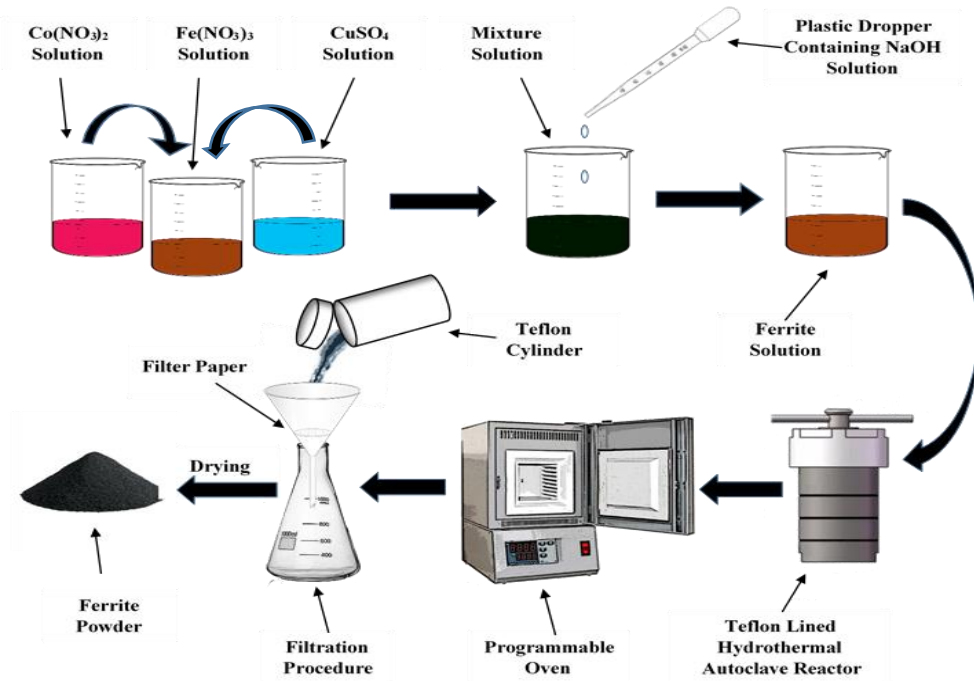


Fig.1: Experimental set up of the hydrothermal synthesis technique.

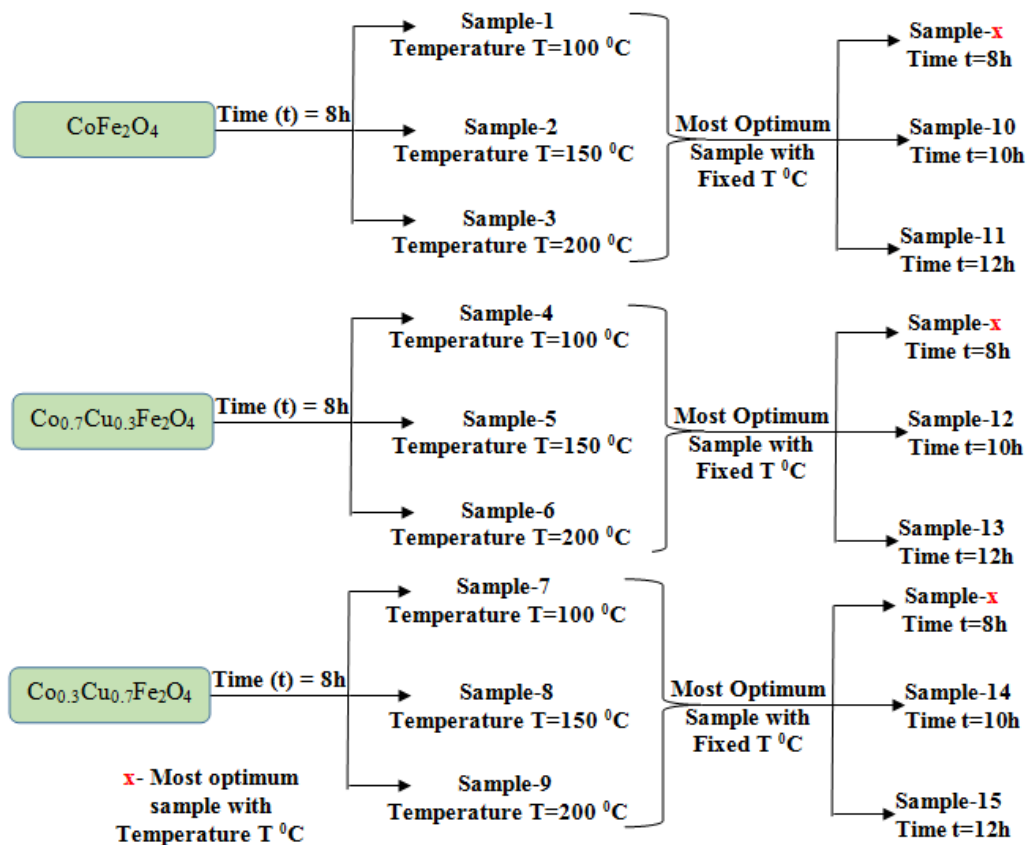


Fig.2: The diagram of the hydrothermal synthesis conditions.

Then next step is to choose synthesis conditions of the three ferrite sample ($x=0, 0.3, \text{ and } 0.7$) of most

optimum temperature (T) and time (t) that provide us smallest average particle size after analyzing the XRD

patterns of them, Then fix the chosen temperature and change the time to (10 and 12) hour as showed in the diagram in Fig.1 and named as sample-10 and sample-11 for CoFe_2O_4 , sample-12 and sample-13 for $\text{Co}_{0.7}\text{Cu}_{0.3}\text{Fe}_2\text{O}_4$, sample-14 and sample-15 for $\text{Co}_{0.3}\text{Cu}_{0.7}\text{Fe}_2\text{O}_4$.

3. Characterization

Phase identification using X-ray diffraction (XRD) analysis of the resulting ferrite nanocrystals was done in a X-ray diffractometer (shimadzu LabX XRD-6100) using $\text{Cu K}\alpha$ radiation ($\lambda = 1.5418 \text{ \AA}$). The powders were scanned at a scanning rate of ($0.02^\circ \text{ S}^{-1}$) and in the 2θ range of ($20^\circ - 80^\circ$). The average crystallites size was obtained using Scherrer equation based on the highest peak (311) [9]. Average crystallite size (D), lattice constant (a), and crystal density (dx) have been calculated for the synthesized samples using the following equations: Scherrer equation [16]

$$D = \frac{k\lambda}{\beta \cos\theta} \quad (1)$$

where k is a constant having a value of 0.89 for the cubic structure, λ is the wavelength of the radiation, θ is the diffraction angle and β is the full width at half maximum (FWHM) of the diffraction peak.

Lattice constant (a) calculated from the relation

$$a = d_{hkl} \sqrt{(h^2 + k^2 + l^2)} \quad (2)$$

where d_{hkl} is the spacing between two crystal planes

The crystal density (dx) is calculated by using lattice parameter and the following relation: [17]

$$dx = \frac{ZM_{wt}}{N_A a^3} \quad (3)$$

where: $Z = 8$ is the number of atoms per unit cell, M_{wt} , N_A and a are the molecular weight, Avogadro's number and lattice constant, respectively.

Results and discussion

XRD studies were carried out in order to get an idea of the crystal structure of the synthesized $\text{Co}_{1-x}\text{Cu}_x\text{Fe}_2\text{O}_4$ ($x = 0, 0.3, \text{ and } 0.7$). The XRD patterns showed six peaks located between (2θ) angles of 20 and 80 degrees which confirmed the spinel structure of the synthesized samples. The results are summarized in Table 1 and Table 2 in which the average crystallite size (D), lattice constant (a) and intensity of the peak estimated from the diffraction peak of (311) because this crystallographic plane exhibited the maximum diffraction intensity.

Firstly sample 1, 2, 3, 4, 5, 6, 7, 8, and 9 have been examined as mentioned in the diagram to study structural properties and predict what best temperature to synthesize with less particle size. The results are shown in the Fig.3 - I, II, and III which shows the XRD patterns of the synthesized ferrite samples CoFe_2O_4 , $\text{Co}_{0.7}\text{Cu}_{0.3}\text{Fe}_2\text{O}_4$, and $\text{Co}_{0.3}\text{Cu}_{0.7}\text{Fe}_2\text{O}_4$ respectively.

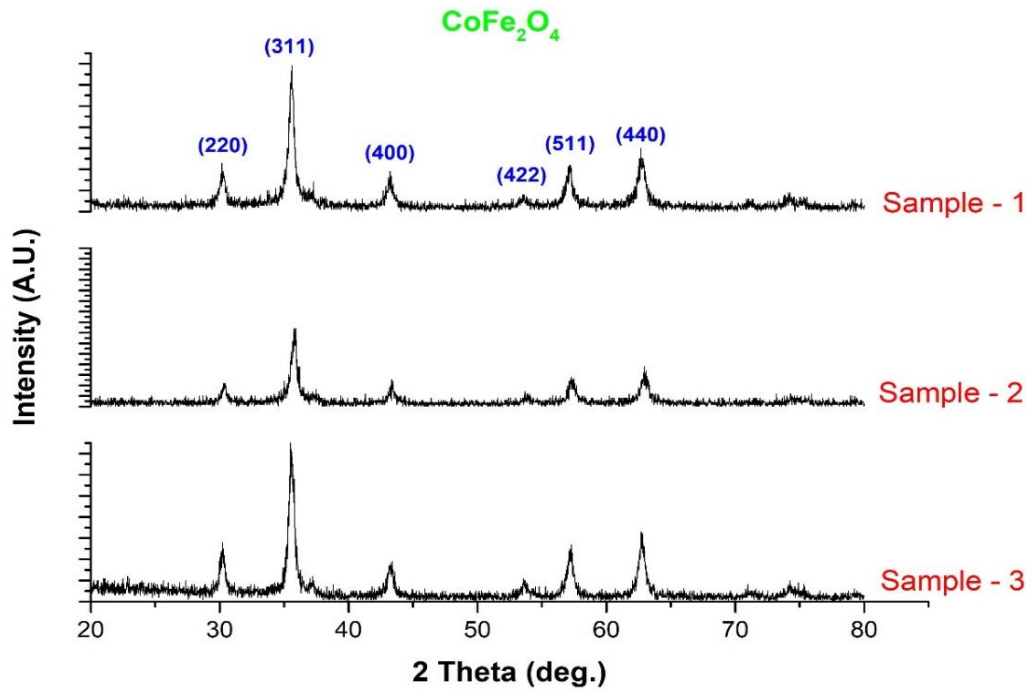


Fig.3-I: XRD pattern of sample - 1 ($T=100^\circ\text{C}$, $t=8\text{h}$), sample -2 ($T=150^\circ\text{C}$, $t=8\text{h}$), sample -3 ($T=200^\circ\text{C}$, $t=8\text{h}$).

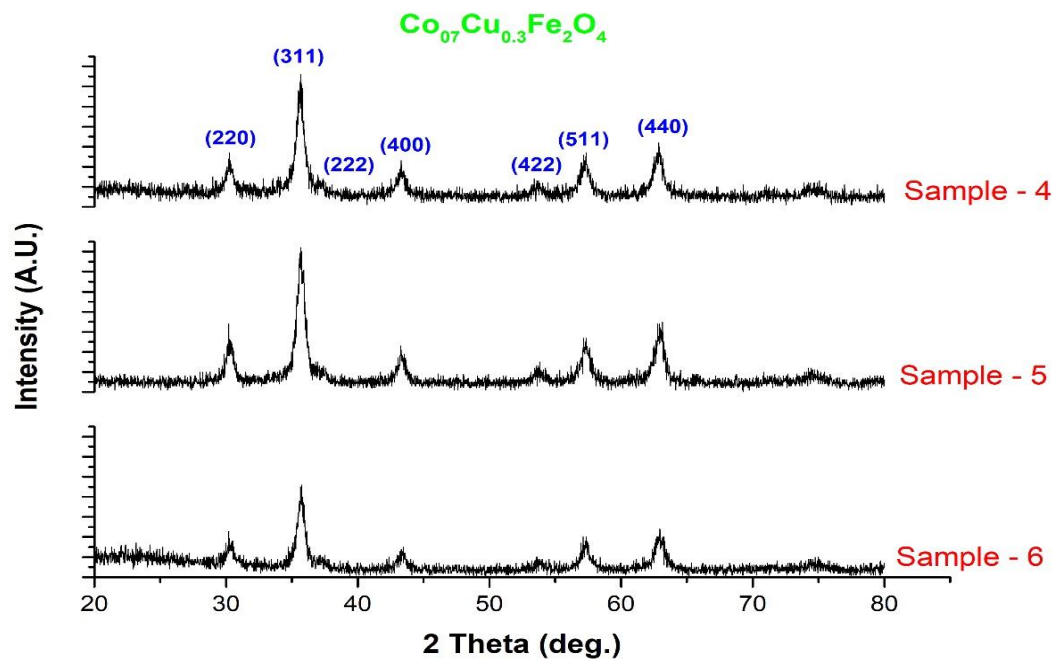


Fig.3-II: XRD pattern of sample - 4 ($T=100^\circ\text{C}$, $t=8\text{h}$), sample - 5 ($T=150^\circ\text{C}$, $t=8\text{h}$), sample - 6 ($T=200^\circ\text{C}$, $t=8\text{h}$).

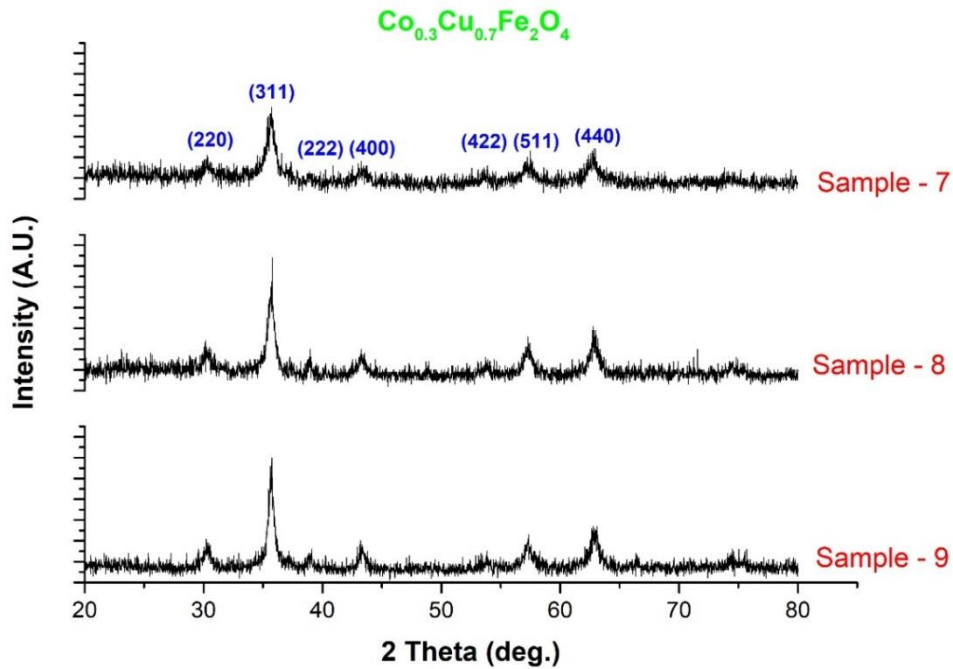


Fig.3-III: XRD pattern of sample – 7 ($T=100\text{ }^{\circ}\text{C}$, $t=8\text{h}$), sample – 8 ($T=150\text{ }^{\circ}\text{C}$, $t=8\text{h}$), sample – 9 ($T=200\text{ }^{\circ}\text{C}$, $t=8\text{h}$).

Table 1: XRD pattern analysis of the nine $\text{Co}_{1-x}\text{Cu}_x\text{Fe}_2\text{O}_4$ ferrite samples. Experimental spacing between crystal plans, lattice constant, average crystallite size and density of powder.

x	Sample	2θ (deg.)	FWHM (deg.)	d_{hkl} (nm)	a (nm)	D (nm)	ρ_x (g/cm^3)
X=0	1	35.58	0.4570	0.2521	0.8361	18.07	5.3317
X=0	2	35.76	0.4900	0.2508	0.8318	16.86	5.4148
X=0	3	35.57	0.4907	0.2521	0.8361	16.83	5.3317
X=0.3	4	35.64	0.6600	0.2516	0.8344	12.51	6.8172
X=0.3	5	35.70	0.6850	0.2512	0.8331	12.06	6.8492
X=0.3	6	35.69	0.6400	0.2513	0.8334	12.91	6.8418
X=0.7	7	35.63	0.71330	0.2517	0.8347	11.58	6.8099
X=0.7	8	35.68	0.62400	0.2514	0.8337	13.24	6.8344
X=0.7	9	35.69	0.5533	0.2513	0.8334	14.93	6.8418

From Table 1 it has been notes that the temperature used in synthesis which provided samples with less particle size is as:

1. For CoFe_2O_4 is $T=200\text{ }^{\circ}\text{C}$.

2. For $\text{Co}_{0.7}\text{Cu}_{0.3}\text{Fe}_2\text{O}_4$ is $T=150\text{ }^{\circ}\text{C}$.

3. For $\text{Co}_{0.3}\text{Cu}_{0.7}\text{Fe}_2\text{O}_4$ is $T=100\text{ }^{\circ}\text{C}$.

So the temperature has been fixed at these conditions and the time changed as shown by the diagram in Fig.4.

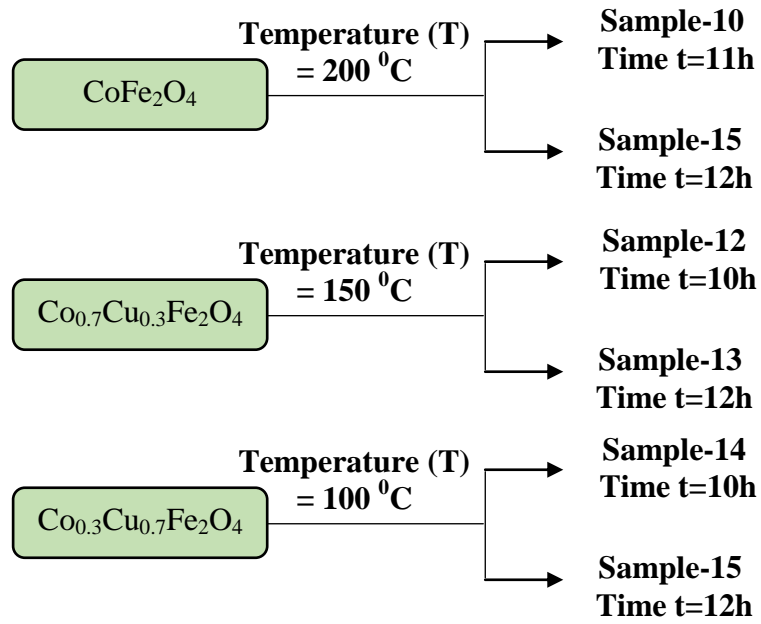


Fig.4: The diagram of the second step hydrothermal synthesis conditions.

Sample 10, 11, 12, 13, 14, and 15 have also been examined and the results are shown in the Fig.5 - I, II, and III which shows the XRD patterns

of the synthesized ferrite samples CoFe_2O_4 , $\text{Co}_{0.7}\text{Cu}_{0.3}\text{Fe}_2\text{O}_4$, and $\text{Co}_{0.3}\text{Cu}_{0.7}\text{Fe}_2\text{O}_4$ respectively.

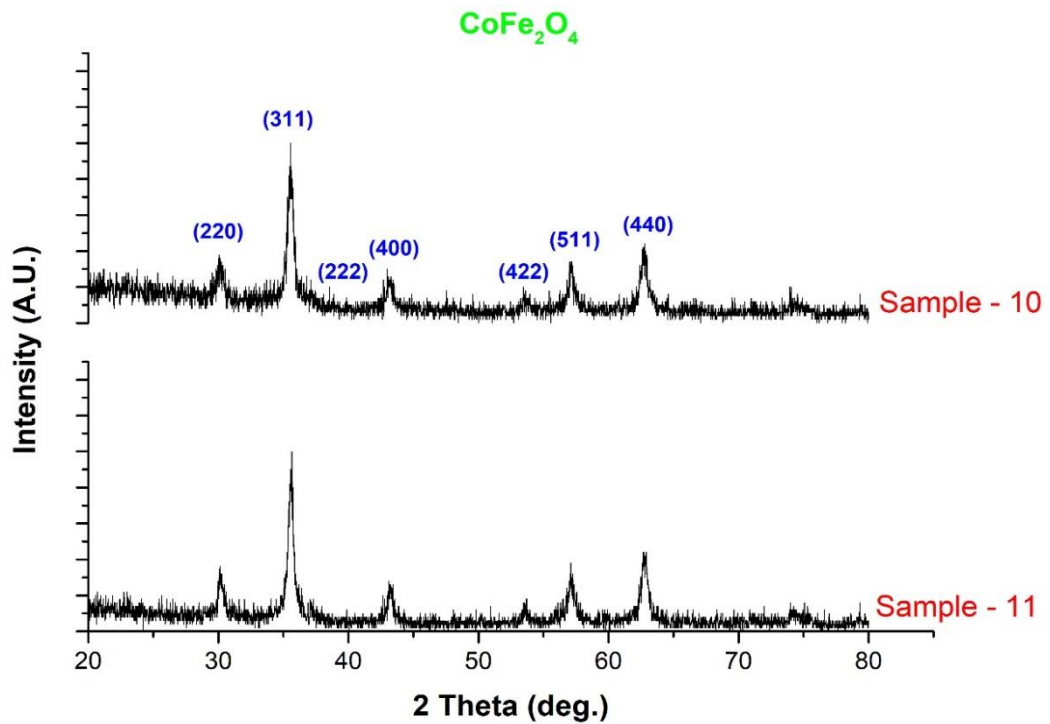


Fig.5-I: XRD pattern of sample - 10 ($T=200\text{ }^\circ\text{C}$, $t=10\text{h}$), sample - 11 ($T=200\text{ }^\circ\text{C}$, $t=12\text{h}$).

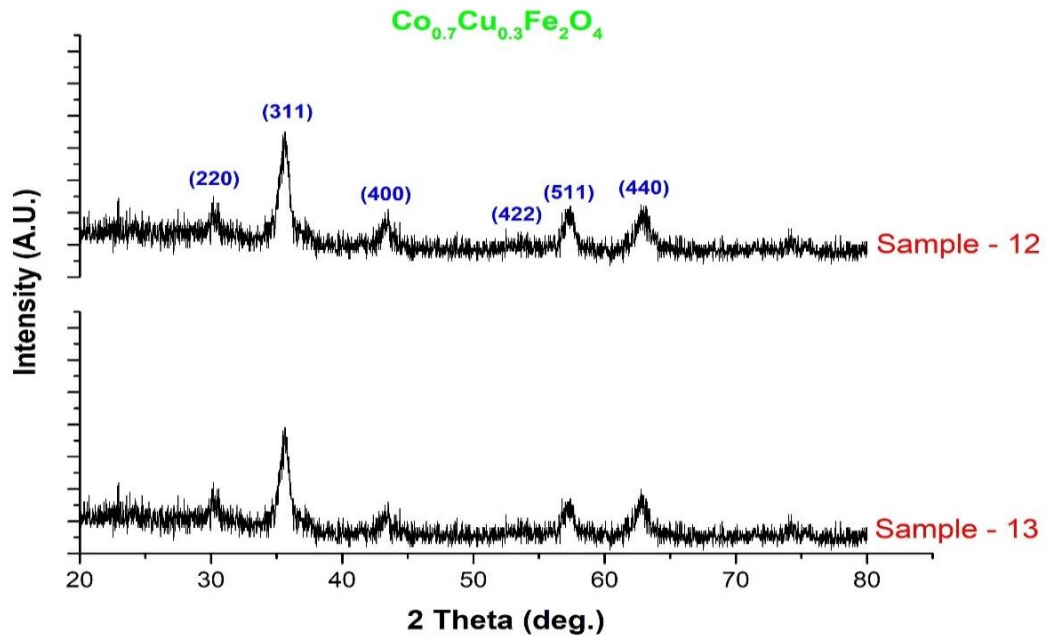


Fig.5-II: XRD pattern of sample – 12 ($T=150\text{ }^\circ\text{C}$, $t=10\text{h}$), sample – 13 ($T=150\text{ }^\circ\text{C}$, $t=12\text{h}$).

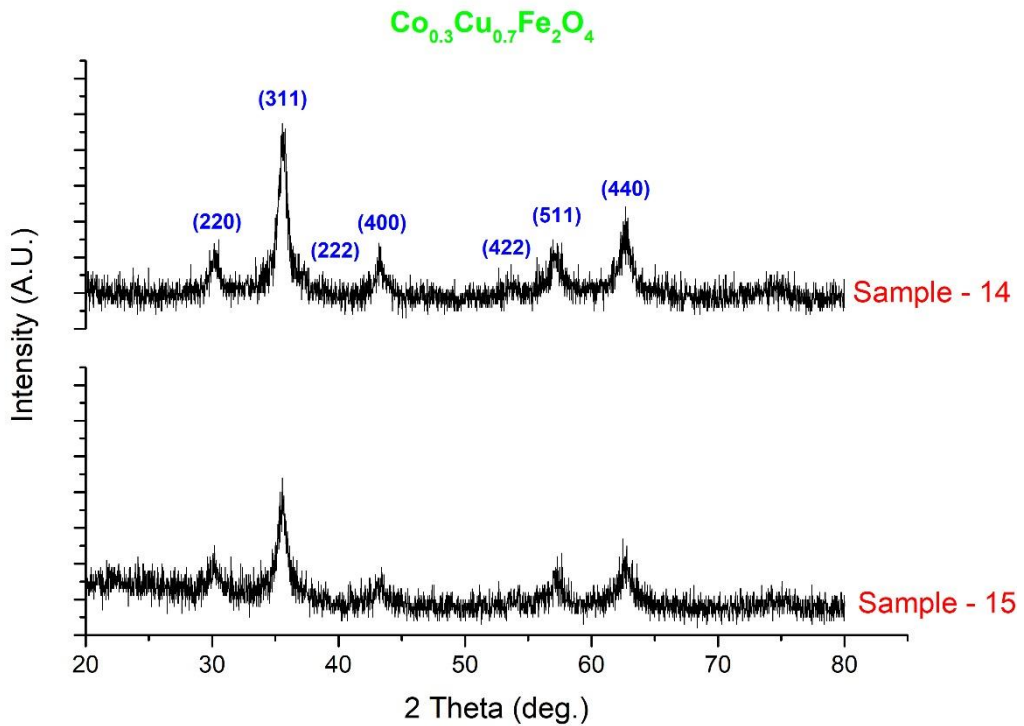


Fig.5-III: XRD pattern of sample – 14 ($T=100\text{ }^\circ\text{C}$, $t=10\text{h}$), sample – 15 ($T=100\text{ }^\circ\text{C}$, $t=12\text{h}$).

Table 2: XRD pattern analysis of the rest $Co_{1-x}Cu_xFe_2O_4$ ferrite samples. Experimental spacing between crystal plans, lattice constant, average crystallite size and density of powder.

x	Sample	2θ (deg.)	FWHM (deg)	d_{hkl} (nm)	a (nm)	D (nm)	ρ_x (g/cm ³)
X=0	10	35.53	0.5267	0.2524	0.8371	15.61	5.3126
X=0	11	35.58	0.4400	0.2520	0.8357	18.77	5.3393
X=0.3	12	35.60	0.7900	0.2519	0.8354	10.45	6.7928
X=0.3	13	35.61	0.7900	0.2518	0.8351	10.47	6.8001
X=0.7	14	35.59	0.8400	0.2520	0.8357	9.83	6.7855
X=0.7	15	35.53	0.7500	0.2524	0.8371	11.01	6.7515

According to average particle size (D) values it has been found that best conditions for synthesize $CoFe_2O_4$ with less average particle size are sample – 10 conditions which are (Temperature T= 200 °C and time t=10h). Synthesized conditions for $Co_{0.7}Cu_{0.3}Fe_2O_4$ are sample – 12

conditions which are (temperature T=150 °C and time t=10h), and synthesized conditions for $Co_{0.3}Cu_{0.7}Fe_2O_4$ are sample – 14 conditions which are (temperature T=100 °C and time t=10h). Table 3 lists structural properties of the desired samples.

Table 3: Structural properties of the chosen ferrite samples extracted from their XRD patterns.

x	Sample	2θ (deg.)	FWHM (deg.)	d_{hkl} (nm)	a (nm)	D (nm)	ρ_x (g/cm ³)
X=0	10	35.53	0.5267	0.2524	0.8371	15.38	5.3126
X=0.3	12	35.60	0.7900	0.2519	0.8354	10.45	6.7928
X=0.7	14	35.59	0.8400	0.2520	0.8357	9.83	6.7855

The variation of lattice parameter and crystallite size with copper ion concentration was shown in Fig.6. The substituted copper ions in cobalt ferrite led to large decrease in lattice constant at x=0 and x=0.3 after this values then the lattice parameter have small

increase in value at x=0.7, while crystallite size decrease with substitution of copper ions this refer to the copper ions replaced with cobalt ions which attributed to the nearly ionic radii of Cu^{+2} ions (0.73 Å) as compared to Co^{+2} (0.71 Å) cations.

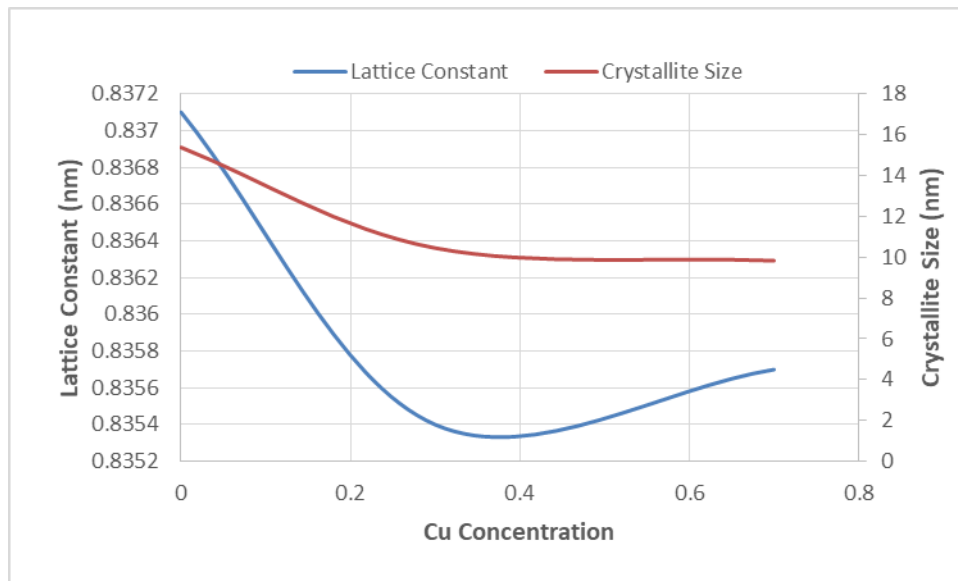


Fig.6: Variation of lattice constants and crystallite size with Cu^{+2} ions concentration.

The effect of Cu content on the variation of crystal density (ρ_x) is depicted in Fig.7. It is obvious from the figure that (ρ_x) is increasing with

Cu concentration due to the increase in the molecular weight of the sample by increasing Cu-content

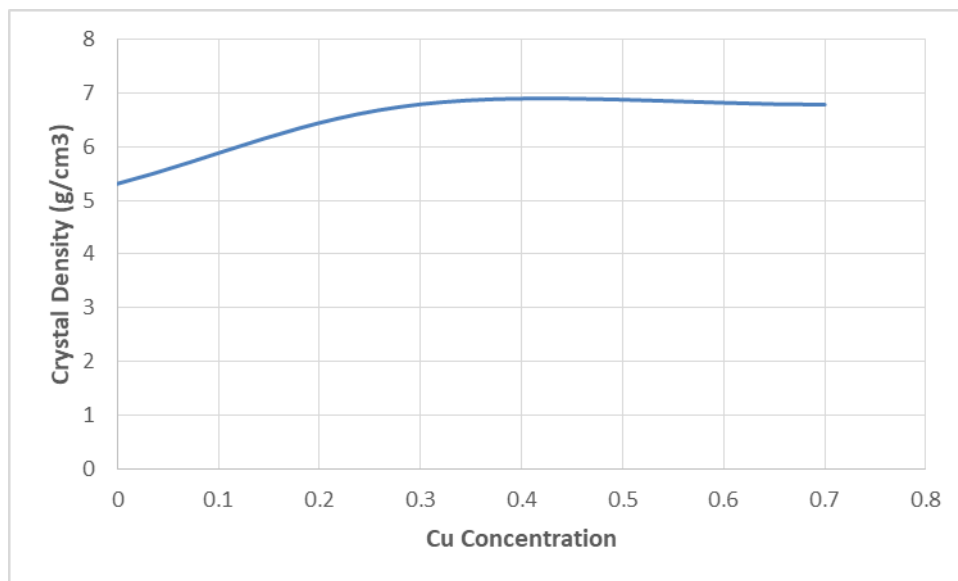


Fig.7: Variation of the crystal density with Cu^{+2} ions concentration.

Conclusions

In conclude cobalt ferrite and copper substituted cobalt ferrite was synthesized using hydrothermal methods. The structural properties of the synthesized materials have been performed using XRD technique. The results showed the formation of the spinal single-phase cubic crystal structure of all samples with average

lattice parameter of 8.36 \AA and we have observed a decreasing of the average particle size with the increasing of Cu concentration. In order to obtain $\text{Co}_{1-x}\text{Cu}_x\text{Fe}_2\text{O}_4$ using hydrothermal method with less average particle size it has been found that hydrothermal conditions listed in Table 4 are the most convenient.

Table 4: Most convenient hydrothermal synthesis conditions of copper substituted cobalt ferrite nanoparticles.

x	Co _{1-x} Cu _x Fe ₂ O ₄	Temperature (°C)	Time (h)
0	CoFe ₂ O ₄	200	10
0.3	Co _{0.7} Cu _{0.3} Fe ₂ O ₄	150	10
0.7	Co _{0.3} Cu _{0.7} Fe ₂ O ₄	100	10

References

- [1] T. Zargar and A. Kermanpur, *Ceram. Int.*, 43, 7 (2017) 5794-5804.
- [2] H. A. Alhadlaq, M. J. Akhtar, M. Ahamed, *Cell & Bioscience*, 5, 1 (2015) 1-11.
- [3] V. Pilati, R.C. Gomes, G. Gomide, P. Coppola, F.G. Silva, F. Paula, R. Perzynski, G.F. Goya, R. Aquino, J. Depeyrot, *J. Phys. Chem. C*, 122, 5 (2018) 3028-3038.
- [4] D. Hong, Y. Yamada, T. Nagatomi, Y. Takai, S. Fukuzumi, *J. Am. Chem. Soc.*, 134, 48 (2012) 19572-19575.
- [5] M. M. Yallapu, S. F. Othman, E. T. Curtis, B. K. Gupta, M. Jaggi, S. C. Chauhan, *Biomaterials*, 32, 7 (2011) 1890-1905.
- [6] S. Mornet, S. Vasseur, F. Grasset, P. Veverka, G. Goglio, A. Demourgues, J. Portier, E. Pollert, and E. Duguet, *Prog. Solid State Chem.*, 34, 2-4 (2006) 237-247.
- [7] T. Hyeon, *Chem. Commun. (Camb.)*, 8 (2003) 927-934.
- [8] Hirthna and S. Sendhilnathan, *Ceram. Int.*, 43, 17 (2017) 15447-15453.
- [9] Z. Zi, Y. Sun, X. Zhu, Z. Yang, J. Dai, W. Song, *J. Magn. Magn. Mater.*, 321, 9 (2009) 1251-1255.
- [10] N. Sanpo, C. Wen, C. C. Berndt, J. Wang, *Adv. Funct. Mater.*, (2015) 183-217.
- [11] M. Bradiceanu, P. Vlazan, S. Novaconi, I. Grozescu, and P. Barvinschi, 52, 66 (2007) 1-2.
- [12] S. C. Goh, C.H. Chia, S. Zakaria, M. Yusoff, C.Y. Haw, Sh. Ahmadi, N.M. Huang, H.N. Lim, *Mater. Chem. Phys.*, 120, 1 (2010) 31-35.
- [13] S. Thakur, S. C. Katyal, M. Singh, *J. Magn. Magn. Mater.*, 321, 1 (2009) 1-7.
- [14] S. I. Abbas, H. T. John, A. J. Fraih, *Indian J. Sci. Technol.*, 10, 21 (2017) 1-6.
- [15] D. Chen, D. Chen, X. Jiao, Y. Zhao, M. He, *Powder Technol.*, 133, 1-3 (2003) 247-250.
- [16] A. K. Zak, W. H. A. Majid, M. E. Abrishami, R. Youse, *Solid State Sci.*, 13 (2011) 251-256.
- [17] Q. Wei, J. Li, Y. Chen, *J. Mater. Sci.*, 36 (2001) 5115-5118.